

RADAR PULSE SHAPE VERSUS OCEAN WAVE HEIGHT

11

A. Shapiro, E.A. Uliana, and B.S. Yaplee

E.O. Hulburt Center for Space Research
Naval Research Laboratory
Washington, D. C. 20390

! N73-15330

The radar height distribution of the vertical ocean surface structure has been measured with a 1 ns radar system from a tower platform. It is shown that the reflecting properties of the ocean biases the mean sea level by about 5% of the significant wave height, and that the radar measured water wave height is reduced by about 6% of the significant wave height. For SWH up to 2 m, it can be assumed that the shape of the distribution is normal and that the mean sea level and water wave height of the observed ocean surface can be directly obtained from the convolved pulse, that is obtained from a high flying altimeter, with accuracies of a few centimeters. Measurements of higher sea states and utilization of an aircraft platform for pulse width limited observations are needed to confirm these preliminary results.

INTRODUCTION

A series of radar measurements over the ocean were made in the spring of 1970 to determine the effect of water waves on extremely narrow radar pulses. The objective of the measurements was to obtain from an analysis of the interaction of a 1 nanosecond radar pulse with the vertical water wave structure quantitative information about the electromagnetic (e-m) ocean height distribution. This information is needed to establish the potential height accuracy and resolution which could be attained with a high resolution satellite radar altimeter over the ocean.

OBSERVATION PROCEDURE AND METHOD OF ANALYSIS

The radar system [1] was installed on the Chesapeake Light Tower (Fig. 1) which is located about 15 miles east of Virginia Beach, Virginia. The radar antennas are about 21 meters above the mean sea surface and sampled a 70 cm diameter ocean surface spot 10 times per second. The ocean wave heights were monitored by three wave staffs separated by about 1.5 m and placed in a delta configuration about the radar illuminated spot (Fig. 2). The wave staff outputs were recorded simultaneously with the corresponding radar return on digital magnetic tape at the 10 Hz rate. For range and reflectivity calibrations, a corner reflector was placed about 3 m above the mean sea surface in the center of the radar beam. A raw data record is shown in Fig. 3 where the wave staff record has been superimposed on the radar return, but shifted in delay, so as to allow the pulse shape of the radar return to be seen more clearly. The ocean radar returns provide two independent types of information, the delay variations of the radar echo with time and the amplitude variations for the different delays. These two effects will be analyzed separately.

The radar height of the sea surface is obtained by measuring the differential delay between the peak amplitude of the sea surface and corner reflector radar return with a potential precision of 0.25 ns. It can be seen that the radar height variations correspond very closely to the wave staff record.

The amplitude variations as a function of observed delay is obtained by calibrating and converting each amplitude to a normalized radar cross section and then averaging the normalized radar cross section for each delay. The two effects are then combined to obtain the resultant electromagnetic height distribution or impulse response.

It was found that the observations could be separated into two groups, one representing the lower sea states covering significant wave heights (SWH) from 0.85 to 1.25 m with wind velocities ranging from 0 to 20 knots and higher sea states with SWH from 1.15 to 1.80 m and wind velocities from 20 to 27.5 knots. The basic difference between the two groups was the noticeably increased fine structure in the height distribution for the larger sea state that was superimposed on the basic gaussian distribution.

In the following presentation of the results a typical example of each group will be discussed to indicate the effect of the sea state on the radar returns and their relation to the wave staff data.

WAVE STAFF AND RADAR HEIGHT MEASUREMENTS

When the amplitude variations of the radar return are removed and only the delay of the peak amplitude is plotted as a function of time, the radar and wave staff profiles of the sea surface for a calm and 20 knot wind sea are obtained as shown in Figs. 4a, b. It is seen that for the calm sea (CLT 17) the radar essentially profiles the underlying sea surface due to the small spot size that is produced by the small antenna beam width and the low platform height. For the higher sea state (CLT 7), it is apparent that some of the higher peaks of the water waves are missed by the radar and the peaks are rounded off due to the finite spot size. The effect of this distortion on the height distribution is shown in Fig. 5a, b for the two cases and the corresponding statistical parameters are given in Table 1. For the calm sea, while no significant difference is apparent in the height distribution, there is a decrease of the skewness value from 0.15 to 0.08 for the radar height distribution. For the wind driven sea there is a decrease both in the skewness value and the width of the radar height distribution, which is apparent from the large number of measured heights near the centroid. The reduced skewness and width is probably caused by the finite size of the illuminated spot and the favoring of the lower areas for reflection, as will be shown later. The differential values of the four moments for all the observations are listed in Table 2. It is seen that the shift in height is random, with an average value of less than 1 cm, but that small biases are introduced to the width, skewness, and kurtosis values of the radar height distributions.

The wave spectra for the two cases have been plotted in Figs. 6a, b to provide further comparisons between the radar and wave staff data. The mean frequency and frequency width for the two observations are given in Table 1. Almost no difference is found for the calm sea, but a slight decrease of the mean frequency occurs for the higher sea state with a small higher frequency component appearing in the radar wave spectrum.

OCEAN RADAR IMPULSE RESPONSE

The beam width limited radar response of this experiment can be related to the equivalent pulse width limited radar response from a satellite altimeter through the ocean radar impulse response. This is obtained by multiplying the radar height distribution by the average normalized radar cross section at each height increment. Typical normal radar cross section variations as a function of

delay are shown in Figs. 7a, b and the gradual increase of the normalized radar cross section as the radar wave penetrates the deeper layers of the water wave structure was noted for all the observed sea states. The slope of the reflectivity curve varied between 3 to 10 cross section units per nanosecond, but no relation between slope and significant wave height or wind velocity could be established. Multiplying the normalized radar cross section with the radar height distributions shown previously for the two sea states, and normalizing the resultant distribution for comparison with the wave staff distribution results in Figs. 8a, b. The weighted distribution is defined as the radar impulse response or electromagnetic height distribution and would correspond to a radar return of an impulse, if a large cylindrical antenna beam were available. The shift of the radar impulse response distribution toward the troughs due to the increasing reflectivity is apparent, but the overall shape has not been greatly affected.

ANALYSIS OF IMPULSE RESPONSE AND RESULTS

The impulse response shown above are typical of 16 observations that covered a range of significant wave heights from 0.84 to 1.81 m (2.77 - 6.05 feet) and wind velocities from 0 to 27.5 knots. To obtain quantitative estimates of the changes of the impulse response distribution relative to the wave staff height distribution, the first four moments of the impulse response distribution were compared with the corresponding moments of the wave staff distribution and the differential values are listed in Table 3.

The shift of the first moment (centroid) is plotted as a function of the significant wave height in Fig. 9. The scatter in the measurements may indicate that the bias is not simply related to the significant wave height, but attempts to relate the spread of the bias to wind velocity, wave spectra skewness, and kurtosis have not been successful. It seems at present that, while other unknown factors of the sea surface structure may contribute to the shift of the electromagnetic centroid, the significant water wave heights are still the dominating parameter in the functional relation. A linear least square fit to the data shows that the bias is about 4.7 percent of the significant wave height with an rms error of ± 5 mm. The results indicate that for significant wave heights up to 2 m the error of the radar height measurements should not exceed 10 cm and, if independent water wave height measurements are available, this error could be further reduced by a first order correction.

To evaluate the potential height resolution of the radar measurements, the width of the impulse response distribution was compared with the width of the wave staff distribution in terms of their equivalent SWH. Again the only relation that could be established was an increasing reduction of the impulse response width relative to the wave staff distribution width as the SWH increased. The results are plotted in terms of the SWH shift in Fig. 10. A linear least squares fit indicates that on the average the equivalent radar SWH is reduced by about 6 percent of the geometric SWH with an rms error of ± 1.4 cm.

The skewness values appeared to be random with an average value of about 0.15 for the wave staff distribution and 0.1 for the impulse response.

The radar kurtosis values were slightly smaller than the corresponding geometric kurtosis values.

Summarizing the results of the impulse response analysis, it is concluded that for small significant wave heights (up to 2 m)

1. the basic normal height distribution is preserved in the radar measurements,
2. the shift of the electromagnetic centroid is small for low SWH, but increases with SWH and may become significant for larger wave heights, and
3. the narrowing of the impulse response introduces a small error in the derived SWH.

PULSE WIDTH LIMITED PULSE SHAPE

To extrapolate from the beam width limited radar observations to the pulse width limited measurements obtained from satellite heights, the observed impulse responses were convolved with a 1 ns ramp and the resulting pulse rise time is shown in Figs. 11a, b for the two examples of sea state. It is apparent that the fine structure of the impulse response is smoothed out, and that the assumption of a simple gaussian distribution model for the impulse response would introduce little error. For a simple gaussian distribution, the mean delay is obtained at the 50 percent threshold level of the maximum amplitude, and the standard deviation can be obtained by halving the delay difference between the 84 percent and 16 percent threshold level of the pulse rise time. Applying the threshold technique to the observed data, it was found that the fine structure of the impulse response introduces peak errors of less than 1 cm to the radar mean height and radar significant wave height.

MODIFICATION OF SATELLITE ALTIMETER PULSE SHAPE AND DESIGN CRITERIA

The previously shown pulse rise time assumes infinite bandwidth receivers and no noise contribution. The finite bandwidth of a receiver will introduce an additional delay and decrease the slope of the radar return. While the additional delay can be calibrated out, at least to first order, the increased slope will reduce the accuracy if noise is present. While the receiver noise can be reduced by increasing the radar system sensitivity, the basic accuracy is limited by the intrinsic noise due to sea clutter, which is determined by the available integration time for a given spatial resolution. Thus it is desirable to maximize the slope for a given sea state if high accuracy is needed. This means that not only should the receiver bandwidth be larger by at least a factor of 2 than that needed for maximum signal to noise ratio, but also that the transmitted pulse width be small relative to the width of the impulse response or the equivalent significant wave height. The effect of a 10 ns pulse on the slope of the rise time is shown in Figs. 12a, b for the observations shown previously. In this case the pulse width is comparable to the width of the impulse response and the slope is increased by a factor of about 2. Thus for optimum height accuracy, low sea states, narrow pulse widths, and wide receiver bandwidths are necessary.

FUTURE PLANS

Additional measurements are needed to establish whether the behavior of the impulse response as obtained from a fixed platform close to the observed ocean surface can be extended to radar observations from a high moving platform. In addition, data at higher sea states are needed to determine whether the relation between the mean height and significant wave height can be extended to larger significant wave heights and whether the assumption of a simple gaussian model distribution is valid for larger sea states. If the impulse response distribution is sufficiently distorted at higher sea states, it may be possible to discriminate between swell and wind driven waves and thus obtain information on the wind velocity field.

An aircraft experiment is now being planned to fly a 1 nanosecond radar over the observing tower and obtain simultaneous radar measurements so that the assumed ergodic hypothesis, i.e., whether time and spatial water wave distributions are equivalent, can be proven. After the initial calibration of the aircraft data, the moving platform will be used to simulate pulse width limited observations and seek out higher sea states so that the data can be extended to the larger significant wave heights.

ACKNOWLEDGMENTS

The authors wish to thank D. L. Hammond for his helpful discussions on the interpretation of the data and who also designed the radar system. Special thanks are given to K. J. Craig who assembled the radar system and collected the data which made this report possible. The authors also wish to thank J. T. McGoogan and H. R. Stanley of NASA, Wallops Station, Dr. M. Swetnick of NASA Headquarters and J. W. Sherman, III of SPOC for their support of this problem.

REFERENCES

- [1] B. S. Yaplee, A. Shapiro, D. L. Hammond, B. D. Au, and E. A. Uliana, "Nanosecond Radar Observations of the Ocean Surface from a Stable Platform," IEEE Transactions on Geoscience Electronics, Vol. GE-9, pp 170-174, July 1971.

TABLE 1

WAVE STAFF AND RADAR HEIGHT PARAMETERS

FOR OBS. 17 ($h_w = 3.45'$, $v_w = 0$ knot) AND OBS. 7 ($h_w = 5.84'$, $v_w = 20$ knots)

| | Obs. 17 | | | Obs. 7 | | |
|-----------------|-----------|-------|--|-----------|-------|-------|
| | Wavestaff | Radar | | Wavestaff | Radar | |
| \bar{t} (ns) | 32.3 | 32.4 | | 28.9 | 28.9 | 28.9 |
| 2σ (ns) | 3.5 | 3.5 | | 5.8 | 5.8 | 5.5 |
| λ | -0.15 | -0.08 | | -0.19 | -0.19 | -0.08 |
| μ^4 | 2.8 | 2.8 | | 3.1 | 3.1 | 3.0 |
| \bar{f} (Hz) | 0.18 | 0.18 | | 0.24 | 0.24 | 0.23 |
| Δf (Hz) | 0.07 | 0.08 | | 0.13 | 0.13 | 0.11 |

TABLE 2

DIFFERENTIAL MEAN HEIGHT, SWH, SKEWNESS AND KURTOSIS
FOR RADAR HEIGHT DISTRIBUTION

| SWH (m) | Δh (m) | Δh_w (m) ^w | $\Delta \lambda$ | $\Delta \mu^4$ | v_w (knots) | Obs. |
|------------|-------------------|----------------------------------|------------------|----------------|------------------|------|
| 0.84 | 0.004 | 0.018 | 0.11 | 0.02 | 10 NE | 22 |
| 0.88 | 0.015 | 0.006 | -0.07 | -0.13 | 5 NE | 20 |
| 0.88 | -0.02 | 0.024 | 0.15 | -- | 15 SE | 24 |
| 0.92 | -0.006 | -0.006 | 0.13 | 0.04 | 20 SE | 25 |
| 0.96 | -0.008 | -0.048 | 0.19 | 0.07 | 14 E | 23 |
| 1.02 | 0.014 | 0 | 0.02 | 0.05 | 20 SSE | 27 |
| 1.04 | 0 | -0.012 | 0.1 | 0 | 0 | 2 |
| 1.04 | 0.018 | 0.012 | 0.07 | 0.05 | 0 | 17 |
| 1.04 | -0.003 | 0.012 | 0.01 | 0.12 | 15 SE | 15 |
| 1.05 | 0.02 | -0.018 | -0.12 | -0.11 | 15 SE | 13 |
| 1.15 | 0.01 | -0.004 | 0.06 | -0.09 | 27.5 S | 26 |
| 1.20 | 0.02 | -0.03 | 0.07 | -0.06 | 12 NNE | 5 |
| 1.26 | 0.016 | -0.04 | 0.08 | -0.2 | 6 ENE | 11 |
| 1.74 | -0.01 | -0.09 | 0.05 | -0.02 | 12 NE | 10 |
| 1.76 | 0.009 | -0.12 | 0.11 | -0.08 | 21 NE | 7 |
| 1.81 | 0.027 | -0.12 | 0.11 | 0.02 | 20 NE | 8 |

TABLE 3

DIFFERENTIAL MEAN HEIGHT, SWH, SKEWNESS
AND KURTOSIS FOR OCEAN RADAR IMPULSE RESPONSE

| SWH (m) | Δh (m) | Δh_w (m) ^w | $\Delta\lambda$ | $\Delta\mu^4$ | v_w (knots) | Obs. |
|------------|-------------------|----------------------------------|-----------------|---------------|------------------|------|
| 0.84 | 0.027 | 0.003 | 0.13 | -0.02 | 10 NE | 22 |
| 0.88 | 0.011 | -0.054 | -0.1 | -0.08 | 5 NE | 20 |
| 0.88 | 0.006 | -0.003 | 0.08 | -0.18 | 15 SE | 24 |
| 0.92 | 0.063 | -0.036 | 0.04 | -0.16 | 20 SE | 25 |
| 0.96 | 0.080 | -0.066 | 0.09 | 0.02 | 14 E | 23 |
| 1.02 | 0.057 | -0.072 | 0.01 | -0.09 | 20 SSE | 27 |
| 1.04 | 0.014 | -0.003 | 0.07 | 0.02 | 0 | 2 |
| 1.04 | 0.057 | 0.003 | 0.07 | -0.11 | 0 | 17 |
| 1.04 | 0.041 | -0.012 | 0 | 0.03 | 15 SE | 15 |
| 1.05 | 0.051 | -0.102 | -0.18 | -0.2 | 15 SE | 13 |
| 1.15 | 0.080 | -0.036 | 0.26 | -0.04 | 27.5 S | 26 |
| 1.20 | 0.033 | -0.042 | 0 | -0.04 | 12 NNE | 5 |
| 1.26 | 0.051 | -0.12 | 0.12 | -0.01 | 6 ENE | 11 |
| 1.74 | 0.054 | -0.102 | 0.08 | -0.07 | 12 NE | 10 |
| 1.76 | 0.084 | -0.132 | 0.13 | -0.13 | 21 NE | 7 |
| 1.81 | 0.12 | -0.222 | 0.14 | -0.05 | 20 NE | 8 |

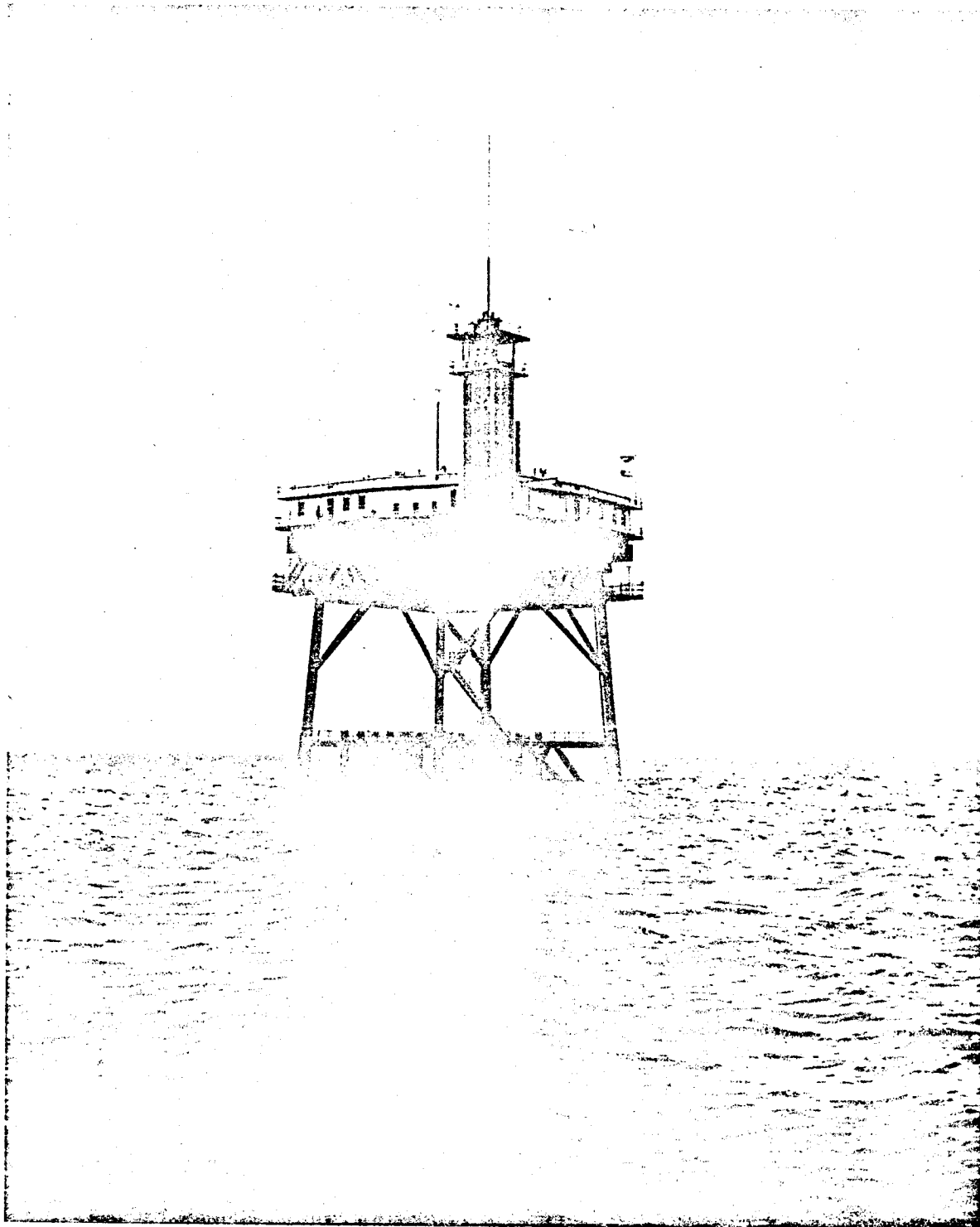


Figure 1. Chesapeake light tower.

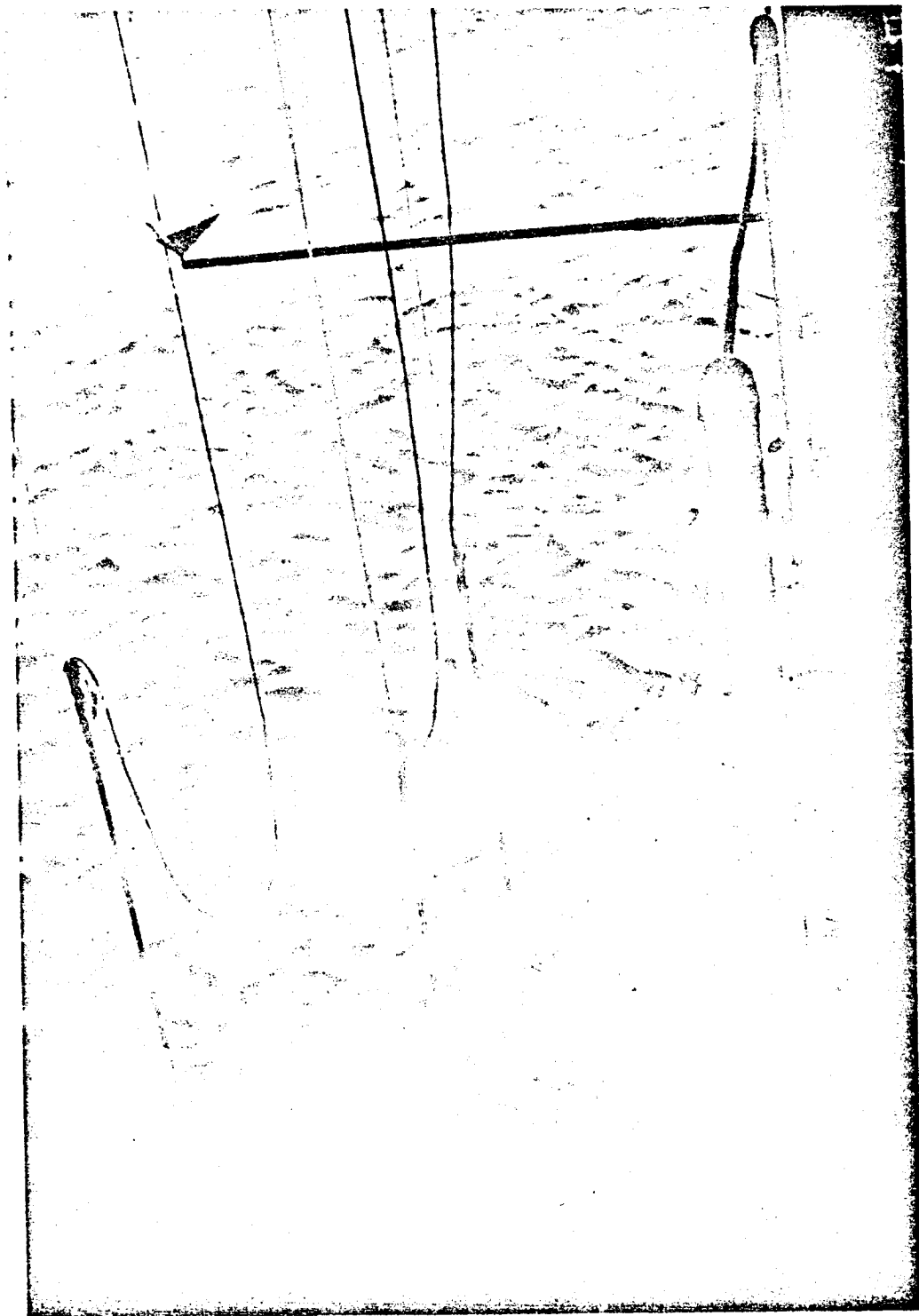


Figure 2. Placement of wave staffs and corner reflector.

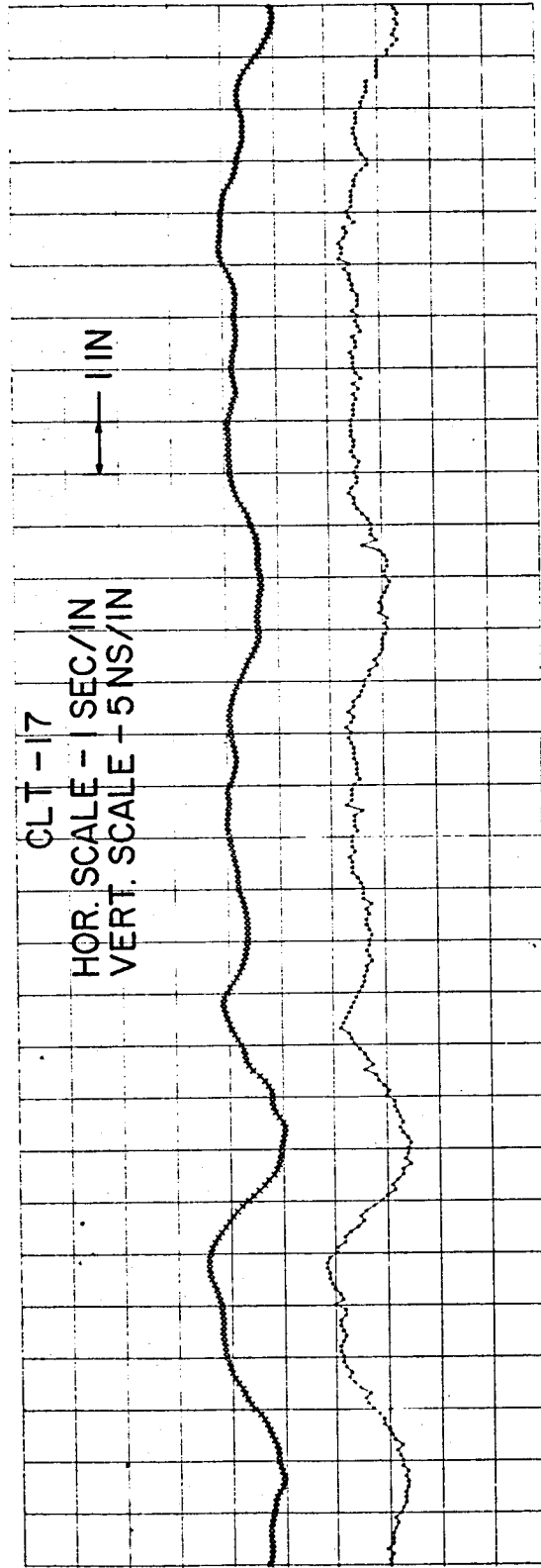


Figure 4a. Water wave profile from wave staff and radar measurements for observations 17 and 7.

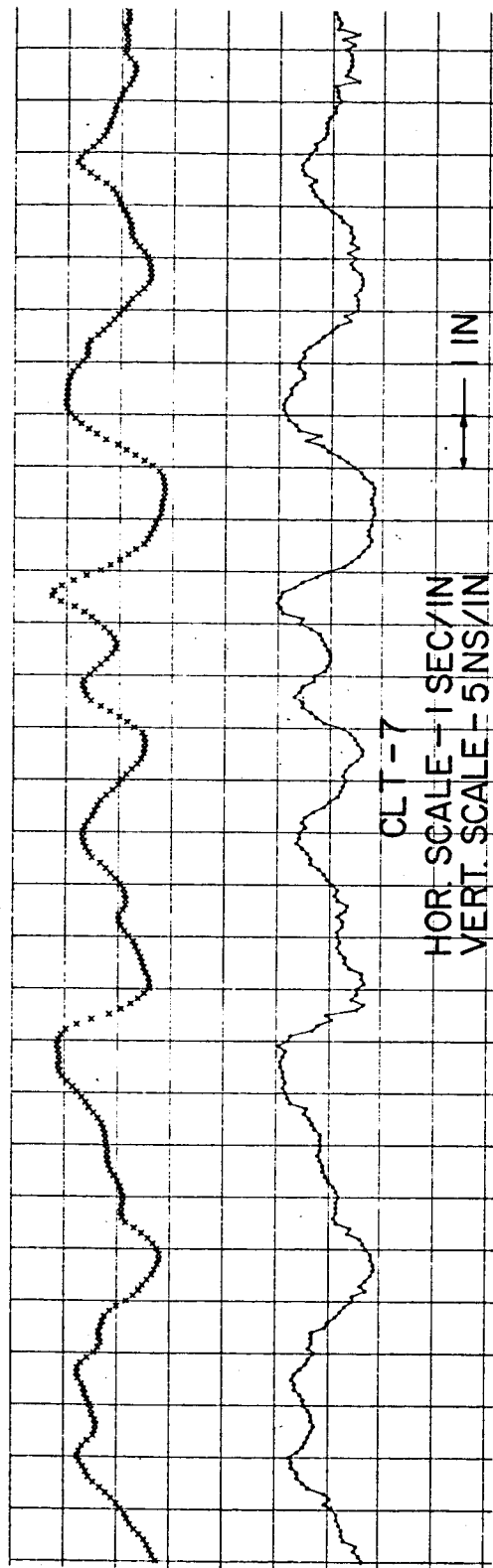


Figure 4b. Water wave profile from wave staff and radar measurements for observations 17 and 7.

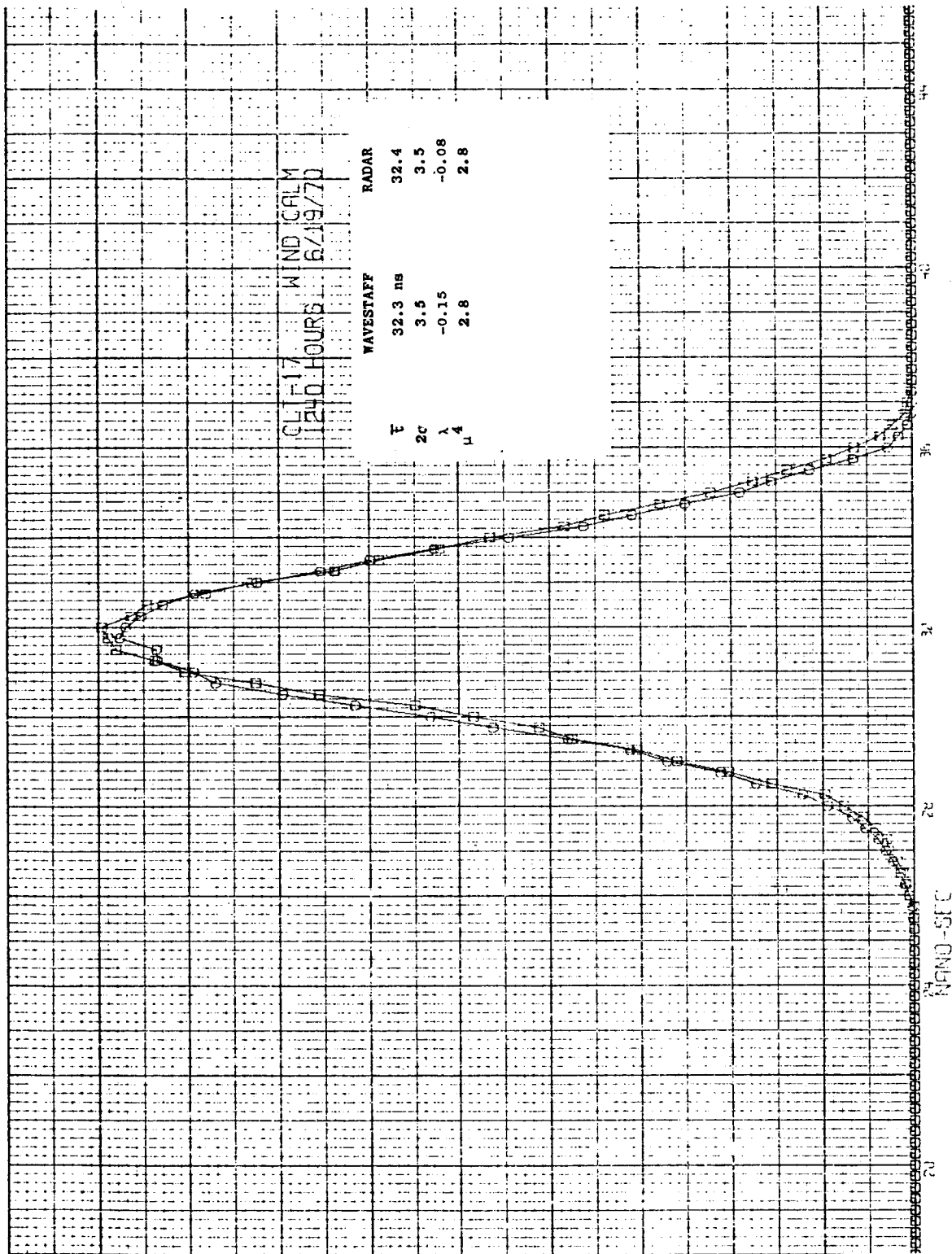


Figure 5a. Wavestaff and direct radar height distribution for observations 17 and 7.

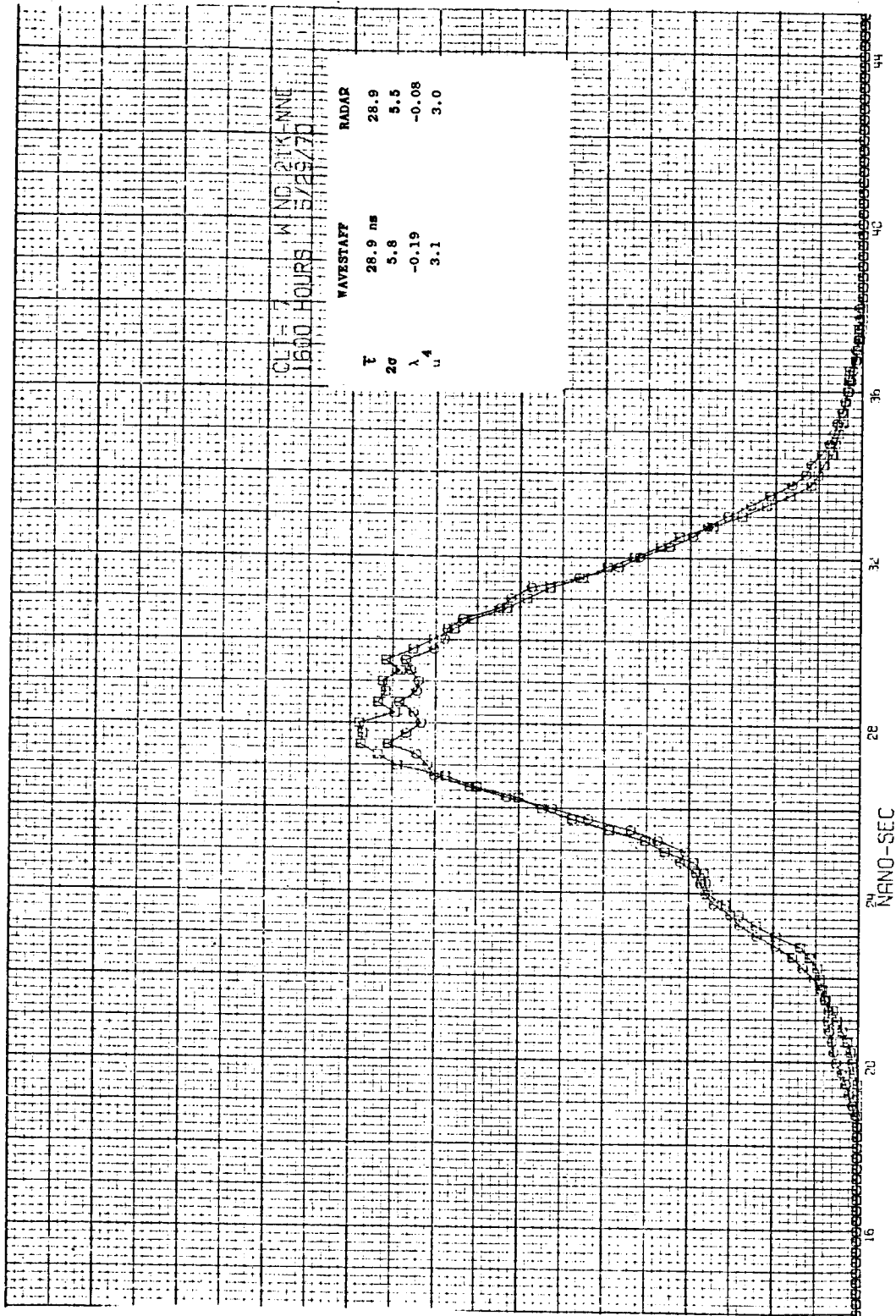


Figure 5b. Wavestaff and direct radar height distribution for observations 17 and 7.

CLT-17 AVG OF FILES 1-6

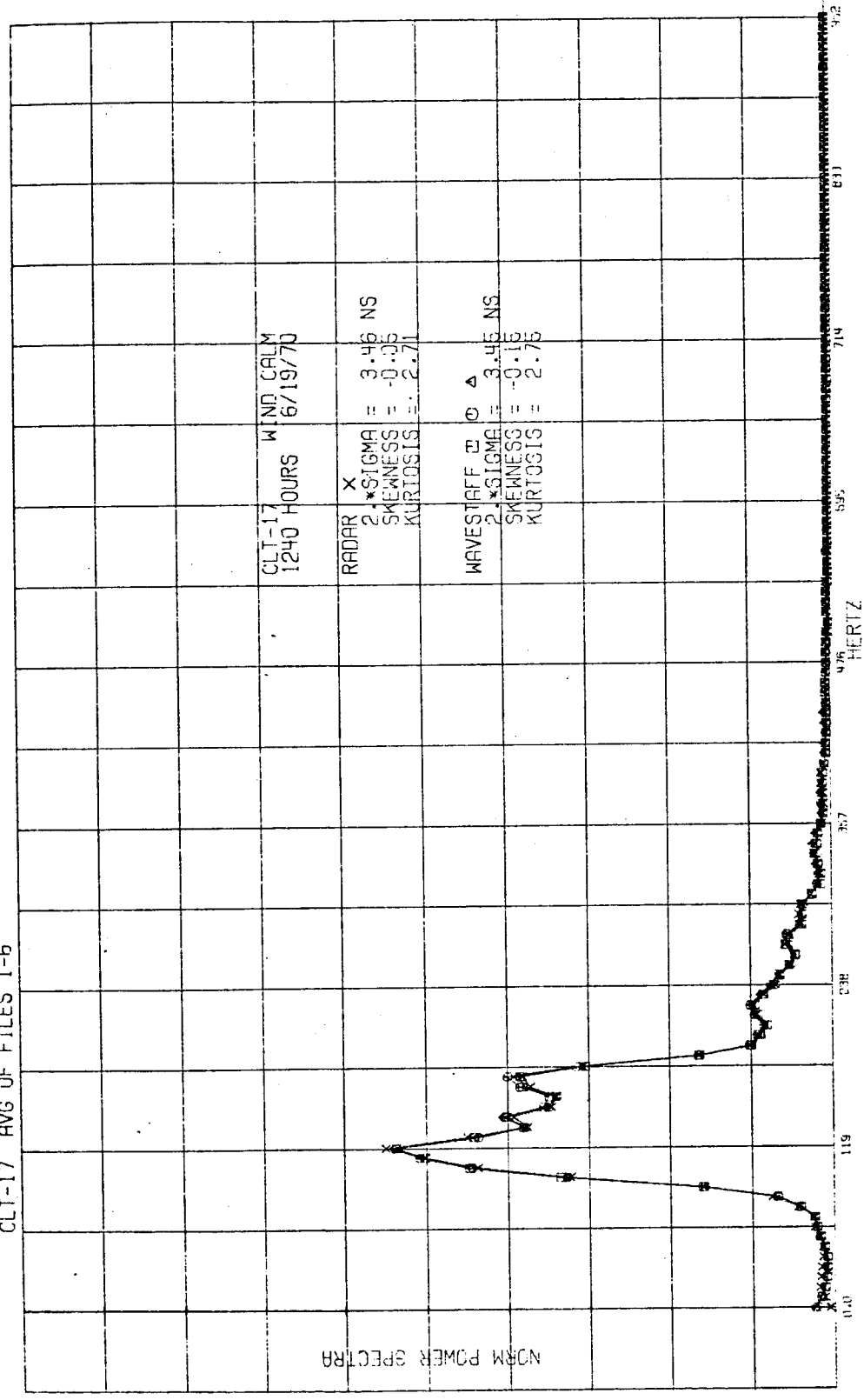


Figure 6a. Wave spectra of observations 17 and 7.

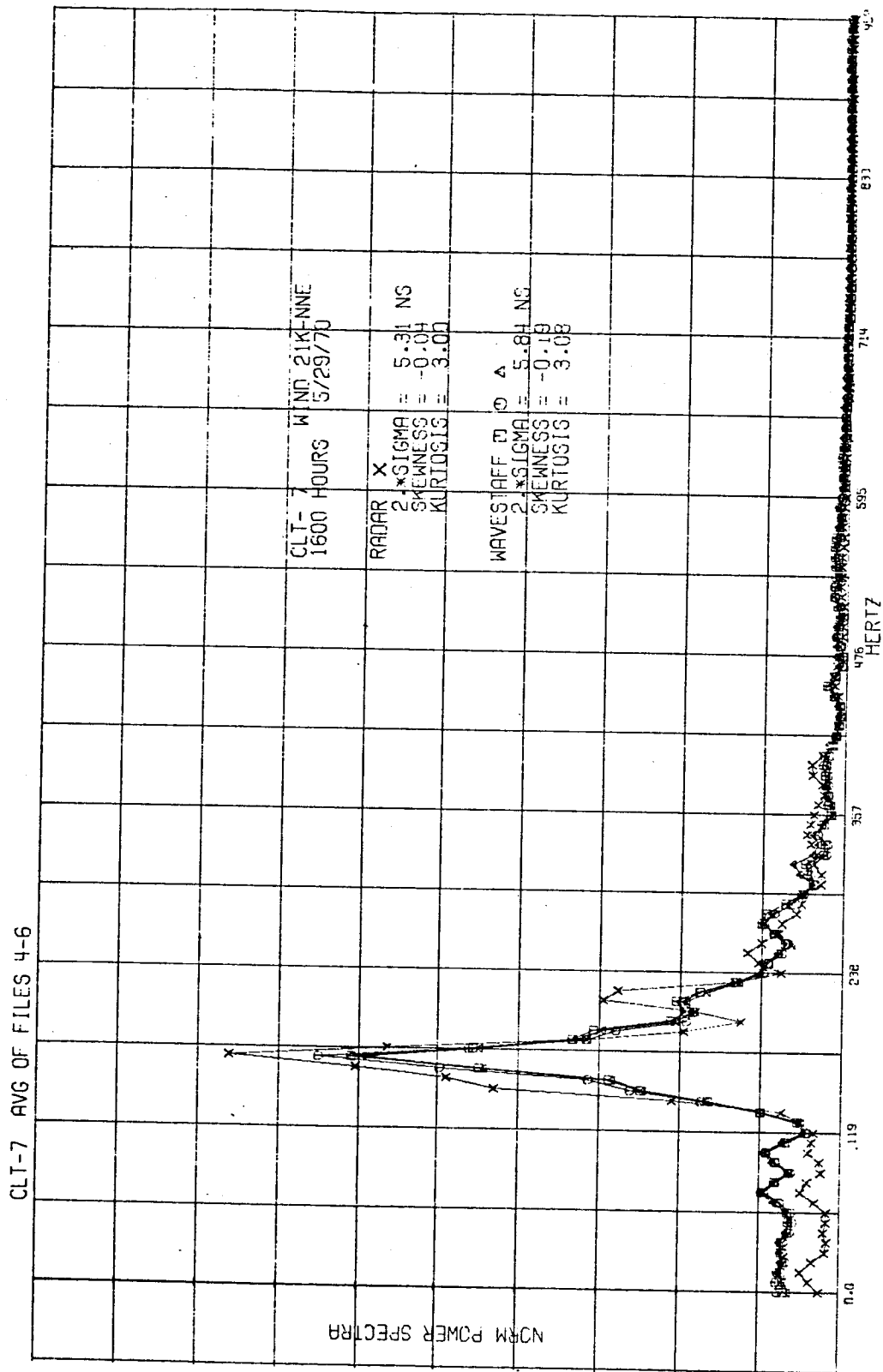


Figure 6b. Wave spectra of observations 17 and 7.

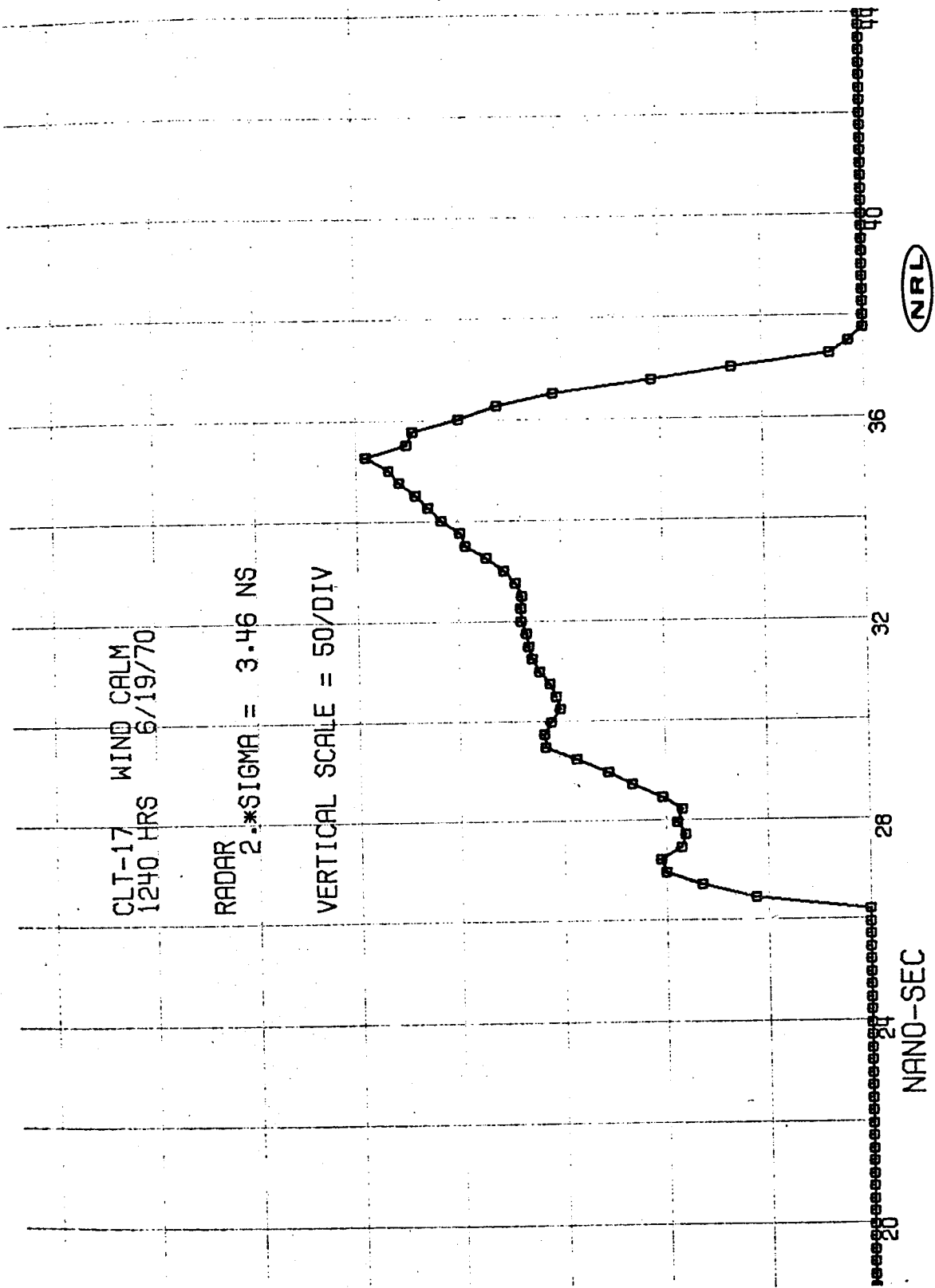


Figure 7a. Reflectivity curve for observations 17 and 7.

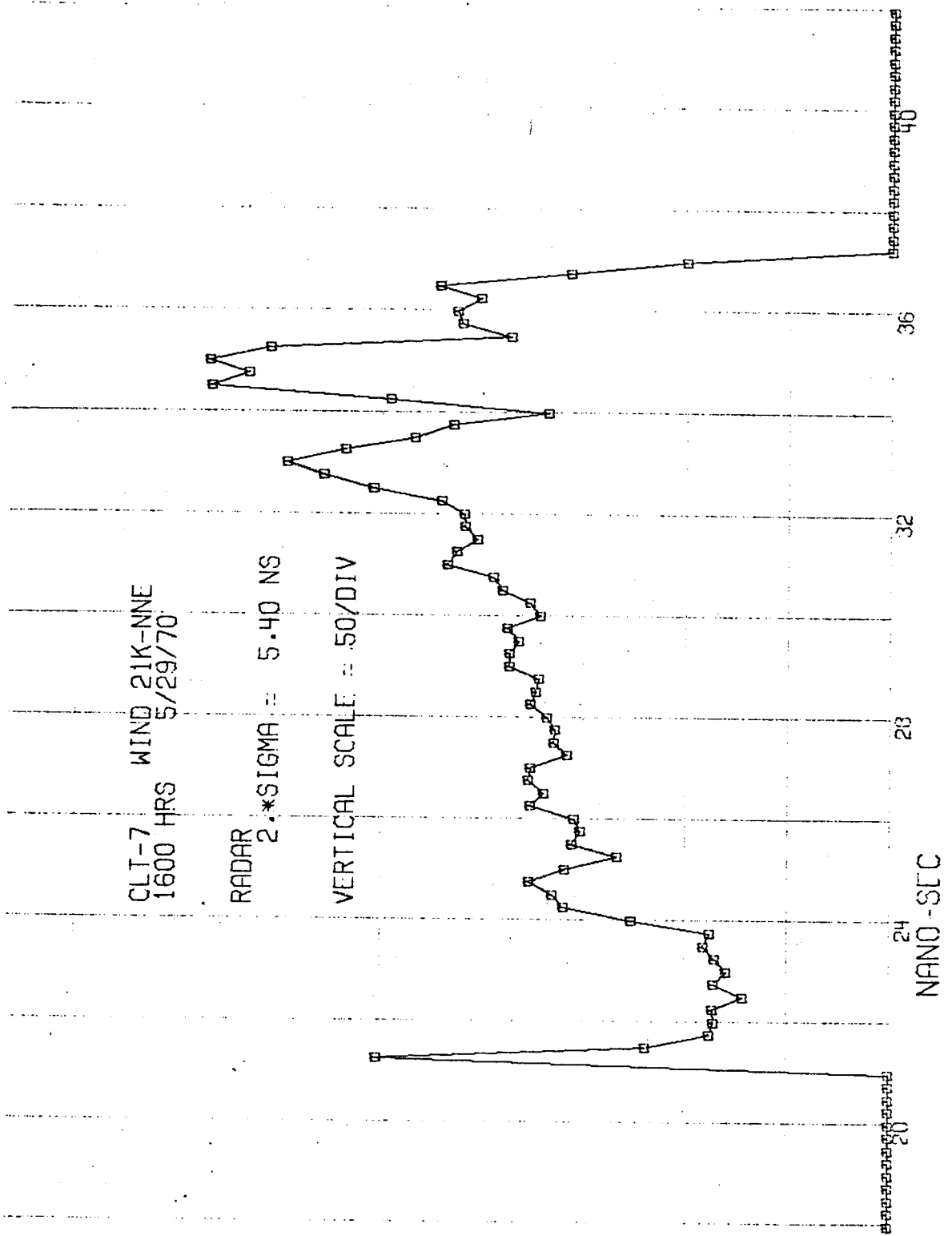


Figure 7b. Reflectivity curve for observations 17 and 7.

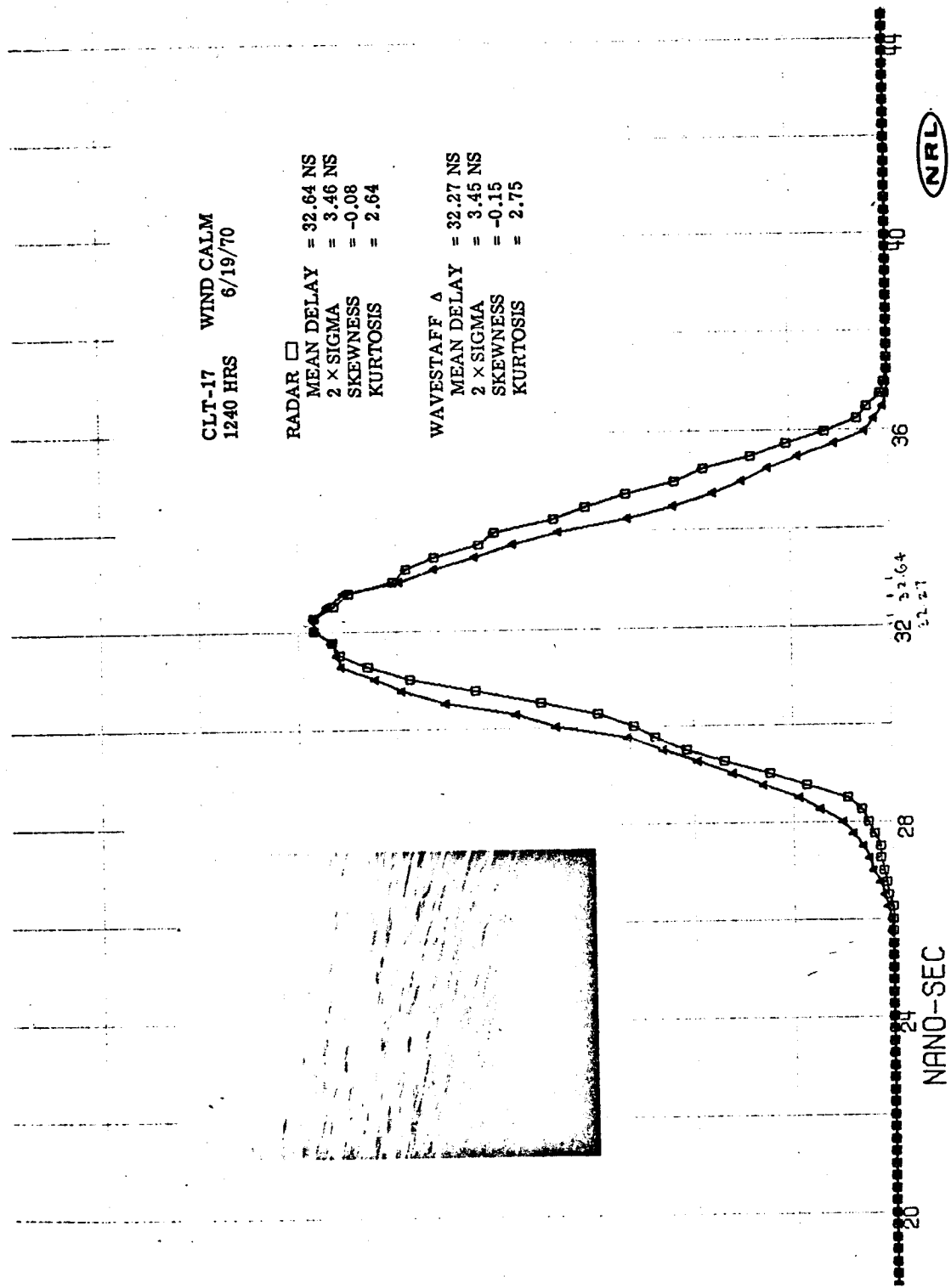


Figure 8a. Radar impulse response for observations 17 and 7.

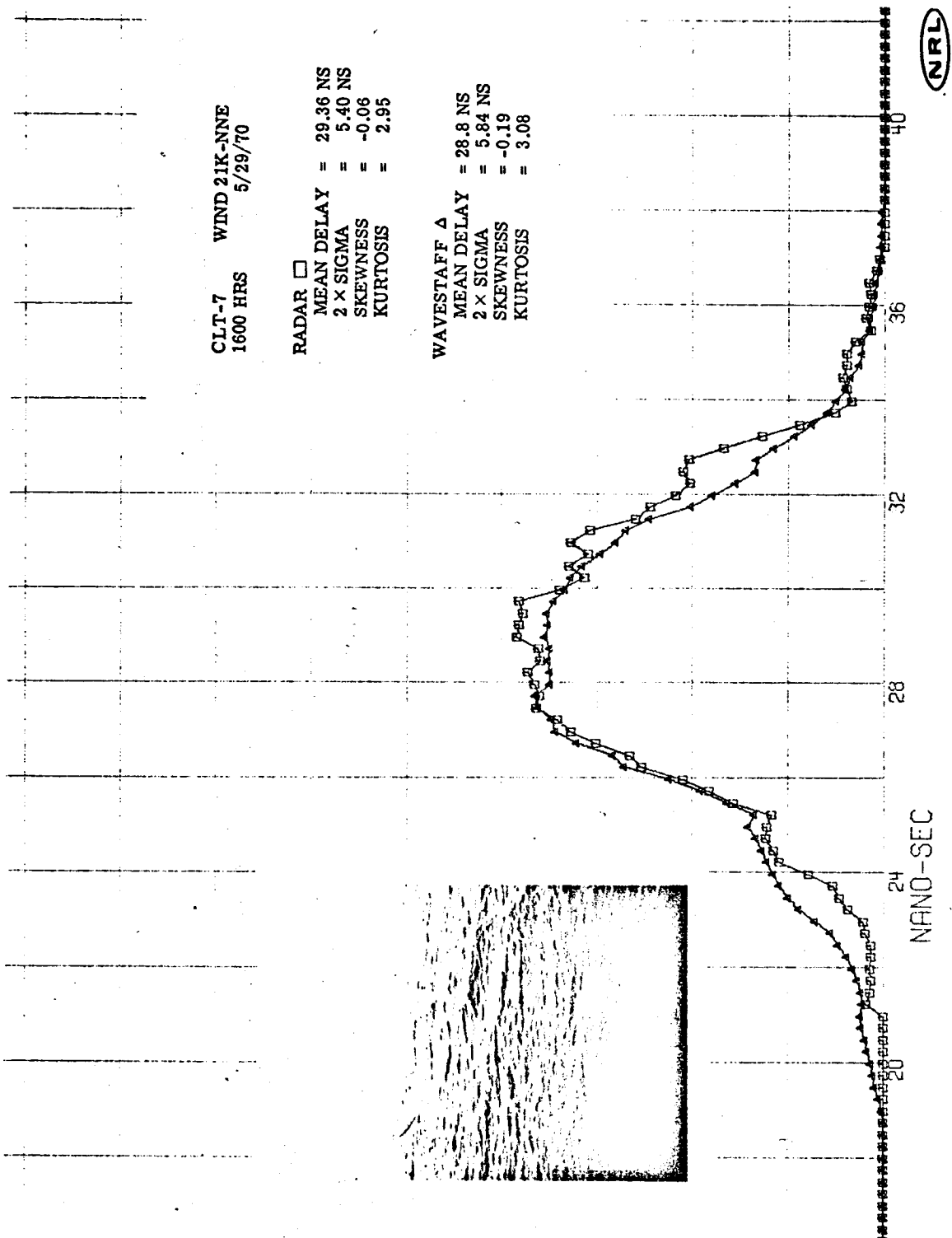


Figure 8b. Radar impulse response for observations 17 and 7.

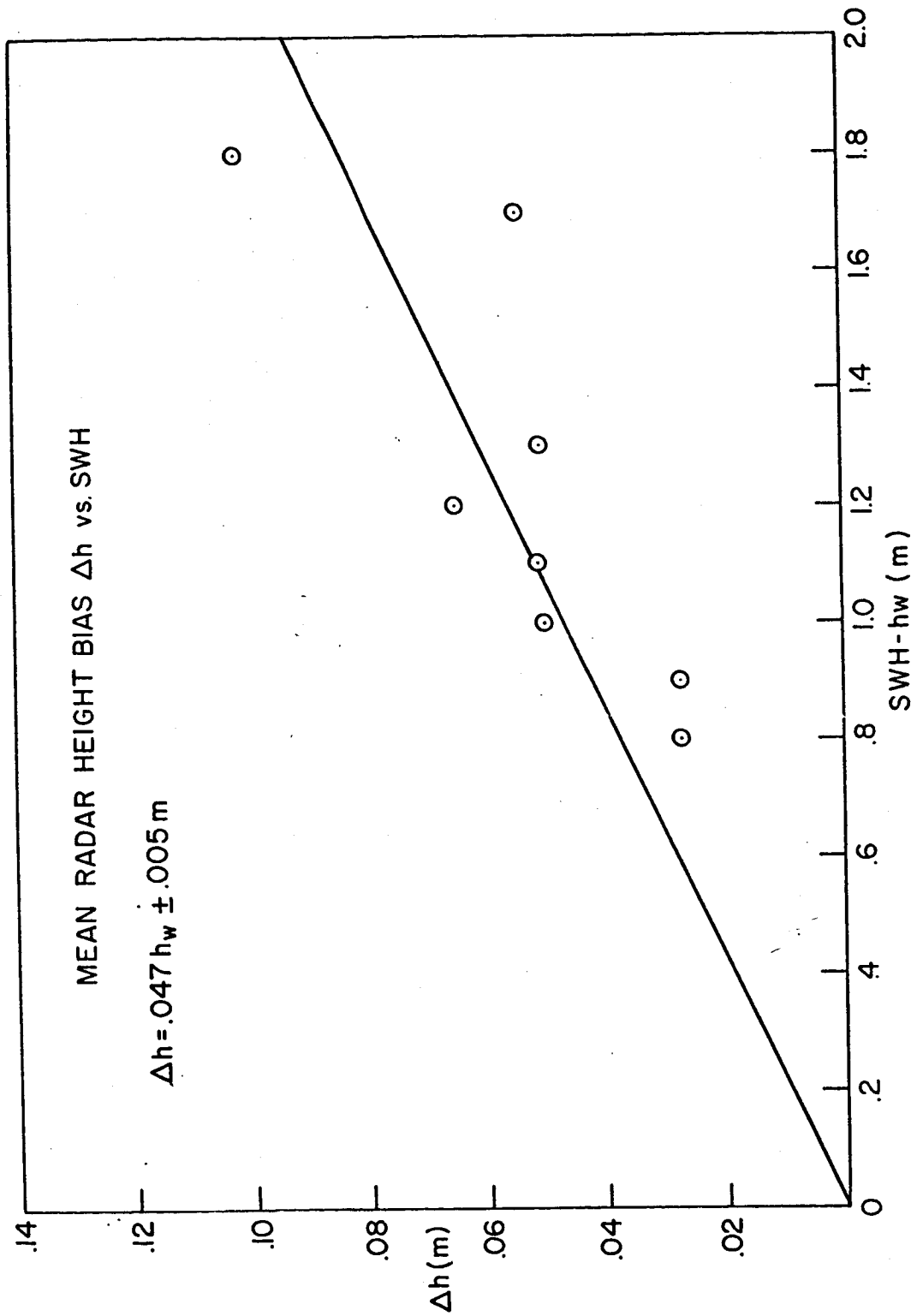


Figure 9. Mean radar height bias versus SWH.

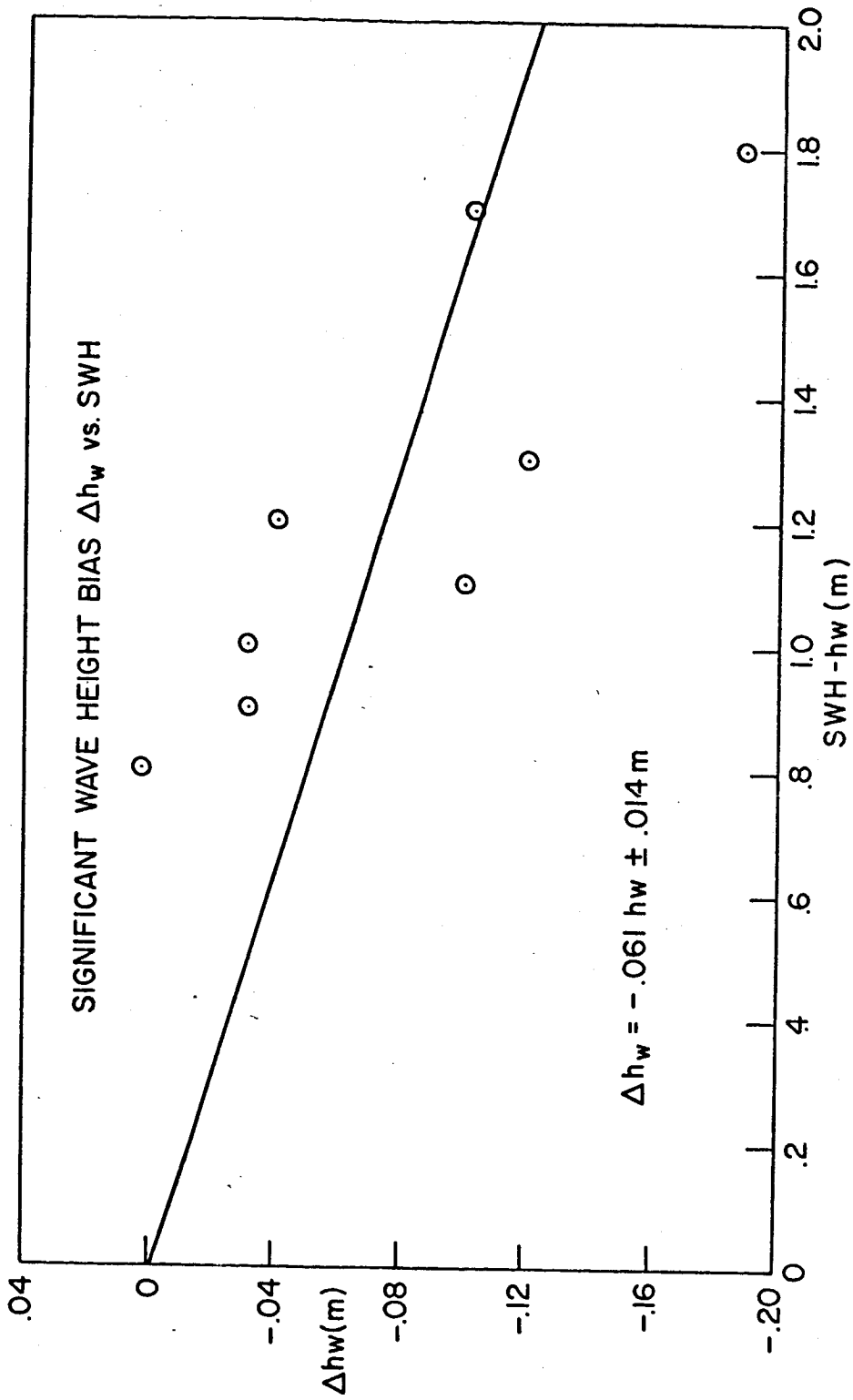


Figure 10. Radar SWH bias versus SWH.

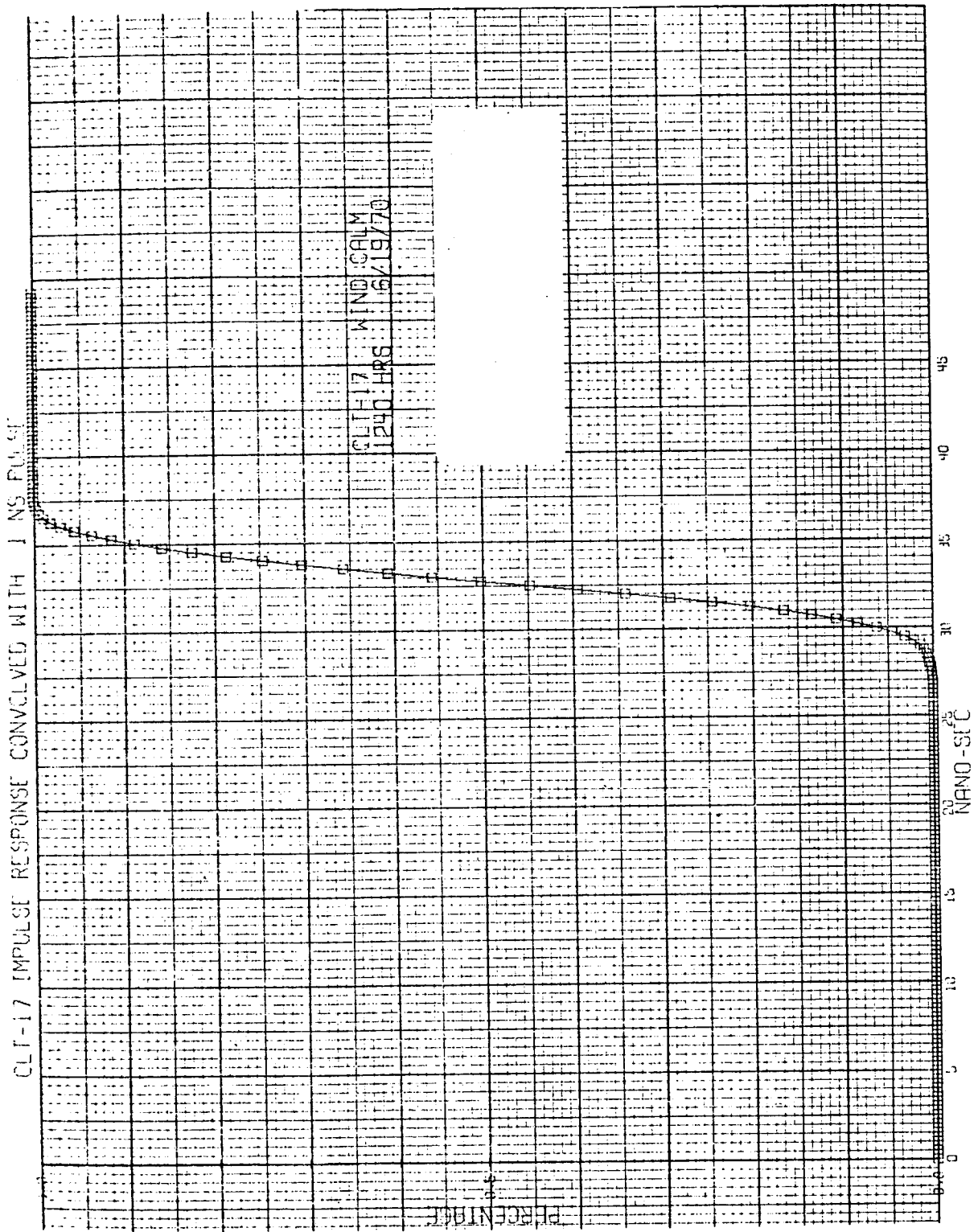


Figure 11a. 1 nanosecond pulse shape for observations 17 and 7.

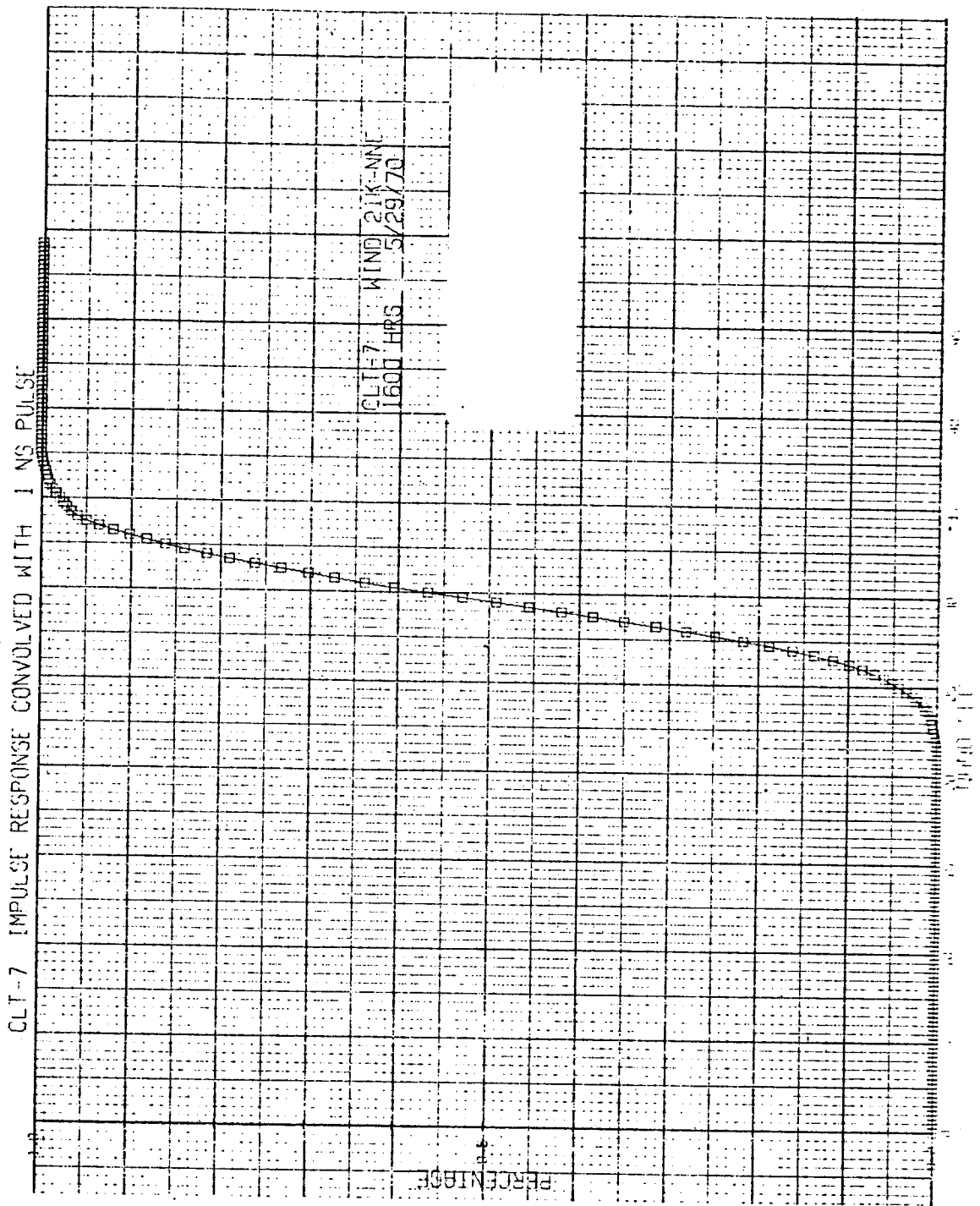


Figure 11b. 1 nanosecond pulse shape for observations 17 and 7.

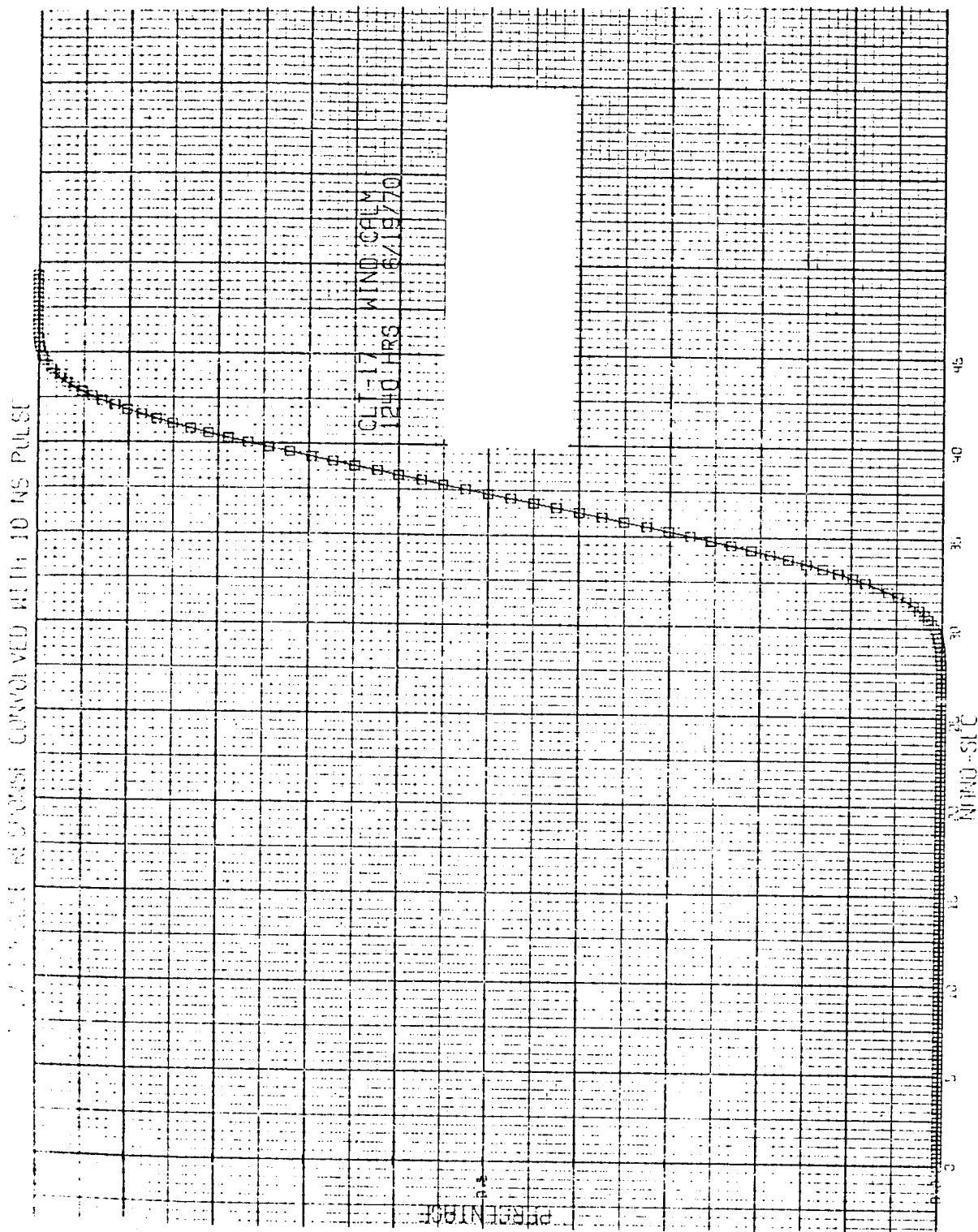


Figure 12a.10 nanosecond pulse shape for observations 17 and 7.

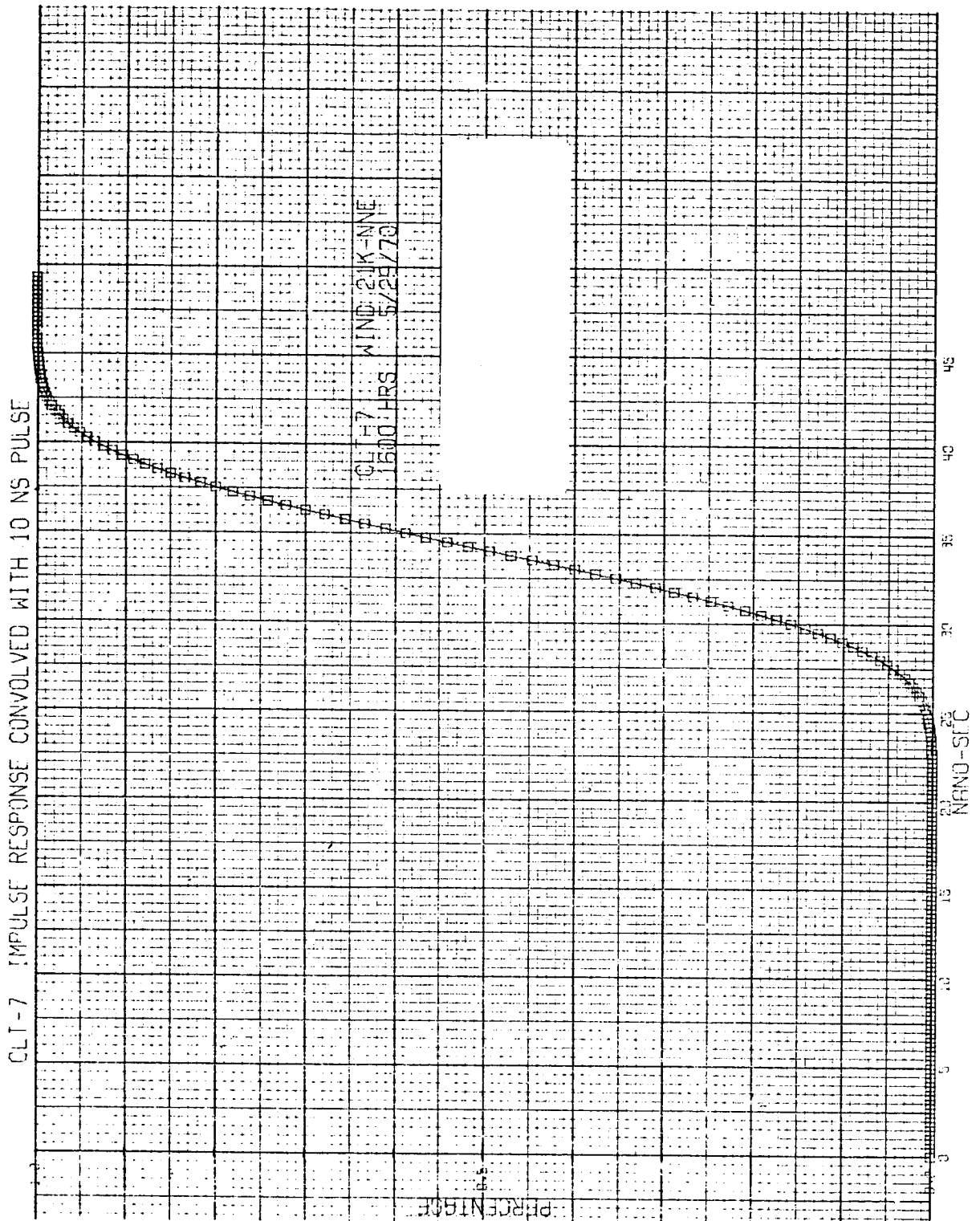


Figure 12b.10 nanosecond pulse shape for observations 17 and 7.